Optical Phase-based Beamformer using MZM SSB Modulation combined with Crystal Polarization Optics and a Spatial Light Modulator

T. Mengual[a], B. Vidal[a], Chr. Stoltidou[b], S. Blanch[b], J. Martí[a], L. Jofre[b], I. McKenzie[c], J. M. del Cura[d]

[a]Nanophotonics Technology Center, Universidad Politécnica de Valencia, Camino de Vera, 46022 Valencia (Spain)

[b]Universitat Politècnica de Catalunya, Campus Nord, 08034 Barcelona (Spain)

[c]European Space Agency, European Space Research & Technology Centre, Keplerlaan 1, 2200 AG Noordwijk (The Netherlands)

[d]SENER, Ingeniería y Sistemas, Aerospace Division, Severo Ochoa, 4, 28760 Tres Cantos, Madrid, (Spain)

Abstract: The performance of a widely tunable phase-based beamformer for phased array antennas using a new technique to cross-polarized the carrier and the sideband, in order to allow the phase control by means of a spatial light modulator, is experimentally demonstrated. The technique relies on the combination of single sideband amplitude modulation (SSB) using a Mach-Zehnder modulator (MZM) and birefringence (to cross-polarized the carrier and the sideband). The architecture has the potential of controlling multiple independent beams simultaneously. The beamformer feeds an 8 elements array showing an insertion loss and a reset speed of around 12 dB and 70 ms respectively. Far-field antenna patterns between 7.5 GHz and 8.5 GHz for nine elevation angles within a rage of ±20º have been measured

showing beam steering capability, amplitude distribution weighting as well as multibeam operation.

***Indexing Terms*:** Optical beamforming, microwave photonics, phased array antennas, spatial light modulator, multibeam.

1. INTRODUCTION

The use of optical beamforming has been studied since the 80's [1-2] because it provides many advantages over microwave and digital beamforming, such as low weight, small size, wideband operation, remoting capability and immunity to electromagnetic interference.

There are three main approaches to optical control of phased-array antennas: true time delay (TTD) systems [3-7], which provide large bandwidth; phase control systems [8], which exploit the parallelism of free-space optics; and a combination of TTD and phase control, which reduces the number of components of pure TTD architectures by providing TTD to subarrays and phase shift between elements of each subarray [9-10].

Additionally, the capability to control a set of independent beams simultaneously would be very interesting since several applications (such as radar, satellite…) require more than one beam at the same time [11-12].

This paper reports experimental results for an optical beamforming network with multibeam capability based on a spatial light modulator and polarization controllers. Measurements of the radiation pattern between 7.5 GHz and 8.5 GHz are provided. In addition, radiation pattern measurements for amplitude distribution weighting and multibeam capability are also presented. The paper is divided into four main sections. Section 2 explains the principle of operation of the beamformer. In Section 3, a description of the proposed

architecture is provided. Section 4 shows the experimental results for beam steering capability, non-uniform antenna amplitude distribution weighting and multibeam operation. Finally, a brief conclusion is summarized in Section 5.

2. PRINCIPLE OF OPERATION

The architecture is based on a nematic liquid crystal spatial light modulator in parallel configuration PA-NLC SLM to provide phase control of the RF signal at each antenna element.

One of the main features of a PA-NLC SLM [13] is that it is possible to control the direction of its molecules alignment by means of the application of an external electrical field. As a result, the polarization component of light parallel to the optical axis of the PA-NLC SLM experiences a different refraction index depending on the applied voltage. In addition, the polarization component of light perpendicular to the optical axis undergoes a constant refraction index. Therefore, if the optical carrier is aligned with this axis, the phase of the optical carrier can continuously be changed. However, if the sideband has an orthogonal polarization, it experiences the constant refraction index. In this way, the phase of the RF signal can be controlled.

In addition, the pixelated PA-NLC SLM structure allows the correspondence between each pixel of the PA-NLC SLM and the antenna elements.

Previous proposals to cross-polarize the optical carrier and its sideband [8-9] were mainly based on acousto-optic modulators (AOM) to modulate a CW laser or the mixing of two tunable lasers with orthogonal polarizations [14]. AOMs offer poor bandwidth, frequency range and modulation index compared to conventional external modulators such as Mach-

Zehnder modulators (MZM) widely available for telecom applications and RF generation from two optical sources is complex. Therefore, a different approach is proposed to cross-polarize the carrier and the sideband. When light is launched to a birefringent material the optical phase of the beam at the output of the device depends on the wavelength,

$$\varphi = \frac{2\pi l(n_e - n_o)}{\lambda} \ . \tag{1}$$

In other words, depending on the wavelength of the incident beam the birefringent material provides different polarization states at the output. Mathematically, this kind of device is represented by the Jones formalism as

$$M = \begin{pmatrix} 1 & 0 \\ 0 & e^{i\varphi} \end{pmatrix}. \tag{2}$$

On the other side, a wave travelling in the z-direction has associated an electrical field, in the xy-plane, which can be expressed as

$$\vec{E}(z,t) = \vec{A}e^{(i\omega t - kz)} \tag{3}$$

where, $\vec{A} = A_x e^{i\delta_x}\hat{x} + A_y e^{i\delta_y}\hat{y}$. Therefore, if the electrical field is represented by a vector,

$$\vec{E} = \begin{pmatrix} E_x e^{i(\omega t - kz + \delta_x)} \\ E_y e^{i(\omega t - kz + \delta_y)} \end{pmatrix}, \tag{4}$$

the intensity of the field can be calculated as follows,

$$I = \vec{E}^{+}\vec{E} \ . \tag{5}$$

The phase shift between two wavelengths spaced a certain frequency, which are travelling through a birefringent material, (f_{RF}) is given by

$$\Delta\varphi = 2\pi f_{RF} DGD \ , \tag{6}$$

where, DGD is the differential group delay introduced by the birefringence ($DGD = \frac{l(n_e - n_O)}{c}$). From (2) and (6) it can be deduced that in order to cross-polarize the optical carrier (f_0) and the sideband (f_0+f_{RF}) and to obtain linear orthogonal polarizations between them, i.e. to obtain a phase shift equal to π, the polarization state of the amplitude modulated optical carrier has to be linear at 45º with the material axis and the DGD needed is $1/(2f_{RF})$ (Fig. 1).

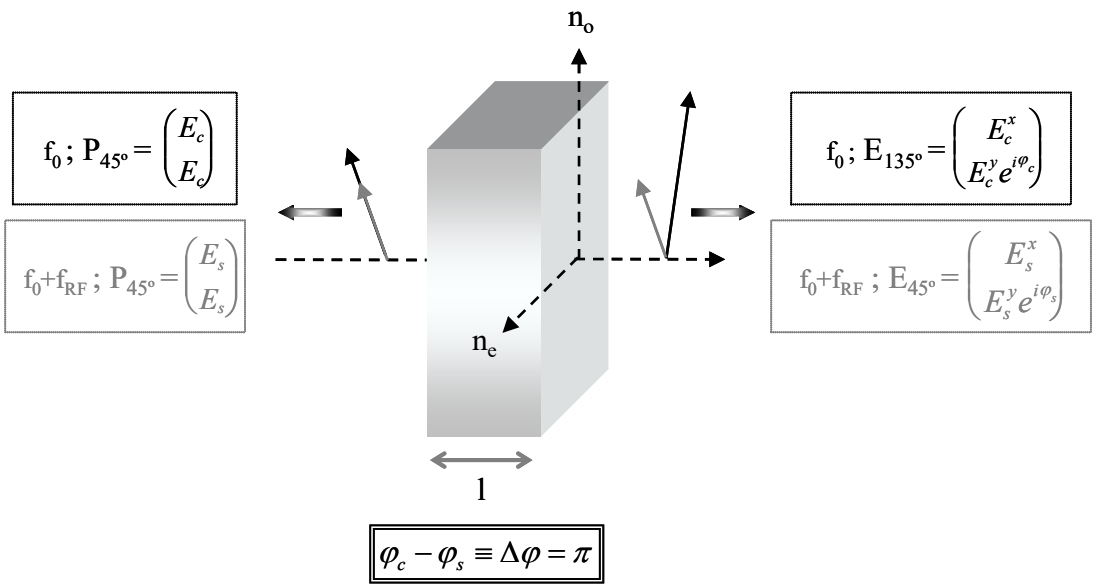

Fig. 1. Polarization at the DGD module input and output.

In order to achieve the phase control by means of a PA-NLC SLM, the axes of the birefringent device and the modulator have to be at 45º. A polarization controller (PC) has to be use to align the carrier polarization along one of the axis of the PA-NLC SLM and the sideband along the other one, as a result, only the carrier or the sidebands will undergo phase modulation. A PC based on a fiber squeezer that rotates around the optical fiber, is the most suitable for this application. Moreover, since two orthogonal signals do not beat at the photodiode it is needed to place a polarizer at 45º behind the PA-NLC SLM in order to

combine the carrier and the sideband in the same state of polarization. The polarizer is represented by the Jones matrix

$$P = \begin{pmatrix} \cos^2(\beta) & \cos(\beta)\sin(\beta) \\ \cos(\beta)\sin(\beta) & \sin^2(\beta) \end{pmatrix} \tag{7}$$

To fully exploit the phase control capability of the PA-NLC SLM, SSB amplitude modulation is needed. Let it be an optical carrier and its sidebands given by the following expressions:

$$\vec{E}_c = \begin{pmatrix} E_c^x e^{i(\omega_c t - kz + \delta_{xc})} \\ E_c^y e^{i(\omega_c t - kz + \delta_{yc})} \end{pmatrix},$$

$$\vec{E}_{s_1} = \begin{pmatrix} E_{s_1}^x e^{i((\omega_c + \omega_{RF})t - kz + \delta_{sx1})} \\ E_{s_1}^y e^{i((\omega_c + \omega_{RF})t - kz + \delta_{sy1})} \end{pmatrix},$$

$$\vec{E}_{s_2} = \begin{pmatrix} E_{s_2}^x e^{i((\omega_c - \omega_{RF})t - kz + \delta_{sx2})} \\ E_{s_2}^y e^{i((\omega_c - \omega_{RF})t - kz + \delta_{sy2})} \end{pmatrix}, \tag{8}$$

the electric field at the photodiode input is

$$\vec{E} = P\, M(\phi_{\text{PA-NLC SLM}})\, R(-\alpha)\, M(\phi_{\text{PC}})\, R(\alpha)\, M(\phi_{\text{D}GD})\, (\vec{E}_c + \vec{E}_{s_1}) \tag{9}$$

in the case of SSB or

$$\vec{E} = P\, M(\phi_{\text{PA-NLC SLM}})\, R(-\alpha)\, M(\phi_{\text{PC}})\, R(+\alpha)\, M(\phi_{\text{D}GD})\, (\vec{E}_c + \vec{E}_{s_1} + \vec{E}_{s2}) \tag{10}$$

in the case of double sideband amplitude modulation (DSB), where R is the rotation matrix corresponding to the PC. Thus, if the polarization state of the sideband and the optical carrier are linear and they are cross-polarized at the PA-NLC SLM input, the RF phase can be obtained from

$$I_{RF} = -E_S^x E_C^y \sin(2\beta)\cos(tw_{RF} + \phi_{\text{PA-NLC SLM}}) \tag{11}$$

in the case of SSB or

$$I_{RF} = -2E_S^x E_C^y \sin(2\beta)\cos(tw_{RF})\cos(\phi_{\text{PA-NLC SLM}}) \tag{12}$$

in the case of DSB, where E_s^x is the x-component of the sideband (note that $\left|E_{s1}^x\right| = \left|E_{s2}^x\right|$), E_c^y is the y-component of the carrier, β is the polarizer angle and $\varphi_{\text{PA-NLC SLM}}$ is the phase shift induced by the PA-NLC SLM. As can be seen, when the optical carrier and the sidebands are linear and cross-polarized, in the case of DSB, there is no phase modulation due to the PA-NLC SLM.

Finally, the capability of the beamformer to control several beams simultaneously is an interesting feature to improve the flexibility and efficiency of the beamforming network. A beamformer of M simultaneous beams requires the use of M optical modulators to translate the microwave signals to the optical domain and the number of pixels of the spatial light modulator has also to be increased by M. To avoid coherent interference is encouraged the use of as many optical carriers of different wavelength as beams.

3. ARCHITECTURE DESCRIPTION

This section describes the beamformer architecture. The block diagram is depicted in Fig. 2. Firstly, two CW-lasers (to implement a beamformer of two independent beams) are amplitude modulated using a dual-drive MZM to generate SSB modulation [15]. Secondly, the signals are coupled, amplified by an Erbium Doped Fiber Amplifier (EDFA) and launched to a DGD module, which cross-polarizes the optical carriers and the sidebands. Next, the signals are demultiplexed using an add-drop multiplexer and each one is split in four channels

of equal length. The signals are launched to free-space, by means of fiber collimators, where a PA-NLC SLM is used to control the phase of each antenna element. After the PA-NLC SLM, a polarizer is needed to combine in a single polarization state, the optical carrier and the sideband; otherwise no signal will be detected at the photodiode. Then, the beams are coupled from free-space into single-mode fibres. The amplitude of each channel is controlled by a Variable Optical Attenuator (VOA). Finally, the signals are photodetected by pigtailed telecom photodiodes. Polarization controllers are used to provide the correct state of polarization to the MZM, the DGD, and the PA-NLC SLM.

As commented in Section 2, the PCs are used to provide the correct state of polarization at the PA-NLC SLM input when the axis of the birefringent device and the modulator are not at 45º. This fact increases the architecture complexity when a large number of antennas elements per beam are used. However, this issue can be overcome using a free space DGD, since no PCs would be need.

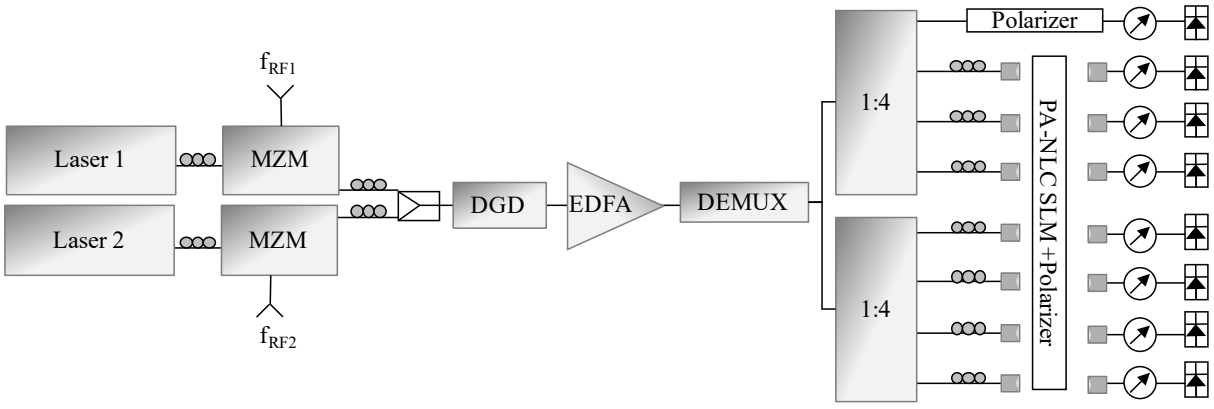

Fig. 2. Block diagram of a two-beams optical beamforming network for controlling an 8-elements antenna array.

4. EXPERIMENTAL RESULTS

Several measurements were carried out to show the feasibility of the architecture. These measurements took place in an anechoic chamber where the receiving antenna was fixed at 5.5 m away from the transmitting antenna (beyond the far-field distance). The transmitting antenna was rotated to measure radiation patterns, as can be seen from Fig. 3.

The beamforming architecture was depicted in Fig. 2. Two lasers, TXP50011AD by Thorlabs, with wavelengths 1550.92 and 1552.52 nm were used as optical sources. The optical power of the lasers was 5 and 7 dBm, respectively, to obtain a similar power at the end of the system. Both signals were amplitude modulated using two DD-MZMs (Fujitsu FTM7937EZ up to 45 GHz and COVEGA Mach 10 060 up to 8 GHz, their insertion loss were (IL) 9 dB at QB) fed by the signal generated by a RF vector network analyser. A fixed DGD module (Prodelay fixed differential group delay module, IL = 2 dB) by General Photonics with a differential group delay of 62.5 ps was used in order to work around 8 GHz

.An optical demultiplexer (WD15SI1 by JDSU, (IL = 1 dB) was used before splitting each signal in four channels (to feed 8 antenna elements). Then, an Optical Delay Line (ODL) was introduced in each one of the 8 channels to compensate for small length differences among parallel branches. After the ODLs (VariDelay^{TM} by General Photonics, IL = 1.5 dB), polarization controllers (PolRite^{TM} by General Photonics, IL = 1 dB) were used to adjust the polarization state of the optical signals to the axis of the PA-NLC SLM. To control the phase of the RF signals, a PA-NLC SLM (CRI-SLM-128-P-NM IL = 3 dB, including collimation loss) and a polarizer were used. A set of 7 x7 collimators were used to collimate seven beams up to 11 cm. One of the channels did not cross through the PA-NLC SLM and the free space polarizer, thus a fiber polarizer was placed in this channel and this path was used as reference. To control the amplitude of the optical signals a set of VOAs (Santec, IL = 1 dB) was

included in the setup. Eight fiber patchcords of 5 meters were used to remotely feed an 8 elements planar antenna. The antenna was in fact an 8x8 planar array but each set of 8 vertical elements were internally connected as a single element to produce fan-beams. A set of eight photodiodes was directly connected to the antenna elements and the setup of Fig. 3 was used to measure the radiation pattern. The optical insertion loss of the entire beamformer was around 12 dB (taking into account an EDFA by Ligthwave2020 with a gain of 19 dB).

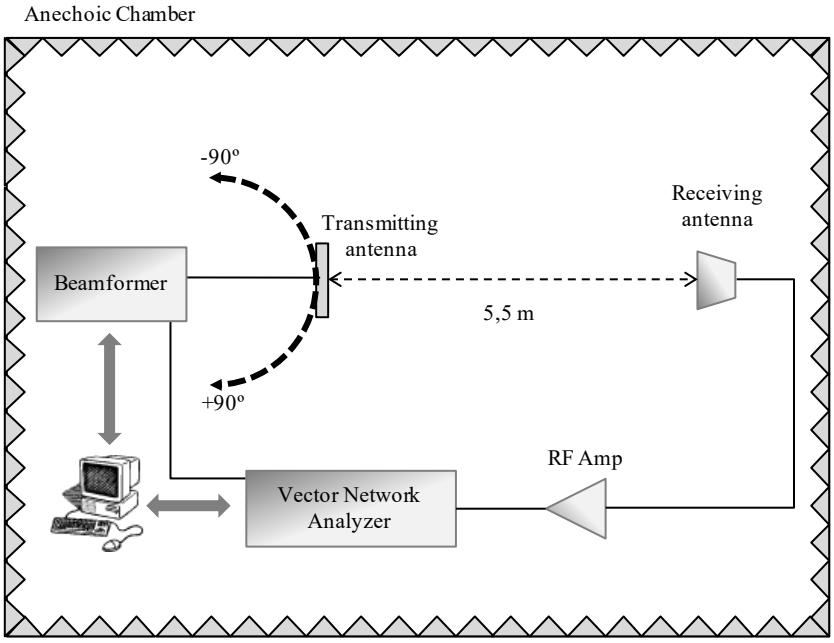

Fig. 3. Scheme of the experimental setup used to obtain radiation pattern diagrams.

4.1. Calibration

In order to carry out the measurements, several adjustments have to be done. Firstly, it has to be checked that the phase shift between MZM drives is $\pi/2$ in order to ensure SSB modulation to fully exploit the phase control capability of the PA-NLC SLM. Secondly, the right state of polarization has to be provided at the DGD input and the PA-NLC SLM by means of the polarization controllers. Finally, the calibration curves (i.e. the phase shift versus

voltage, as shown in Fig. 4) of each channel have to be measured since, the PA-NLC SLM pixels (98μm x 5mm) were divided into 7 sets.

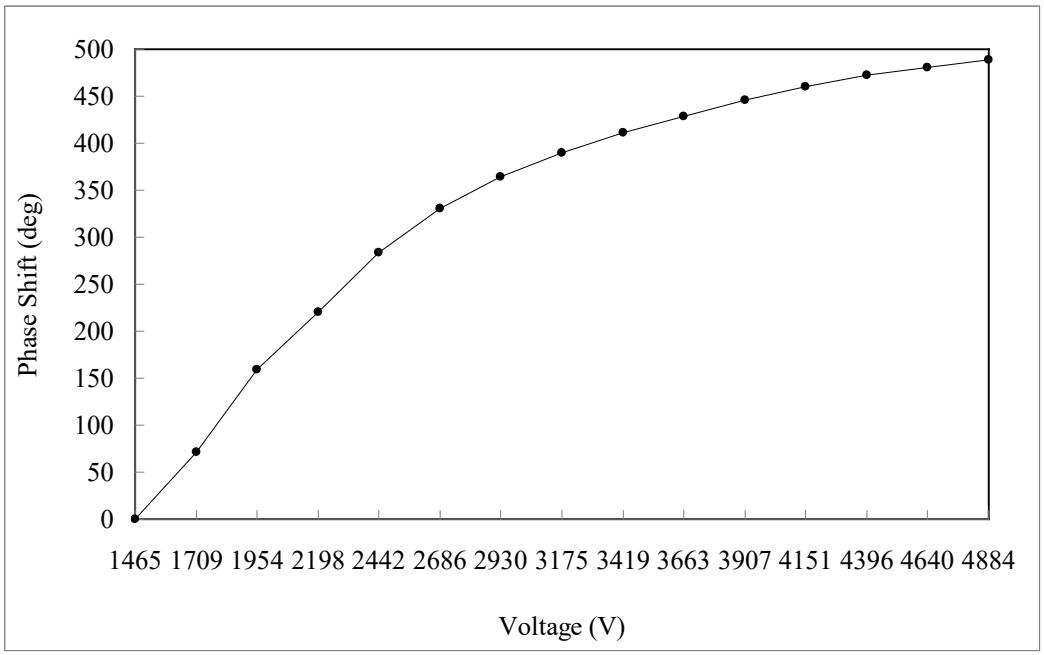

Fig. 4. Phase modulation obtained over 8 GHz signal for one beamformer channel.

As can be seen from Fig. 4, the phase of an 8 GHz tone can be controlled using the PA-NLC SLM over a range of 3π, i.e. a microwave phase shift up to 3π with a response time of 70 ms can be achieved with this device

The DGD was designed to obtain linear orthogonal polarizations between two wavelengths spaced 8 GHz. However, the DGD cross-polarized signals spaced within a range of around 8 ±4 GHz, but in these cases the state of polarization it is not linear as a result, once the calibration curves are measured a change in the f_{RF} leads to an error in the phase shift of the elements antenna if the polarization is not readjusted by the PCs. This effect is not observed in the bandwidth (0.5 GHz) of the experiments carried out.

4.2. Beam Steering capability

The radiation patterns of the 8-elements antenna (with a antenna spacing of 0.8λ) have been measured for different beam steering angles (0º, ±5º, ±10º, ±15º, ±20º) and at five frequencies between 7.5 GHz and 8.5 GHz for a uniform current distribution. Figure 5 shows, as an example, the radiation patterns when the main lobe is steered to -20º with respect to the broadside.

The antenna array radiation pattern can be expressed as

$$\vec{E}(\vec{r}) = \vec{E}_0(\vec{r}) \sum_{n=0}^{N-1} a_n e^{in(kd\cos\theta+\alpha)}, \qquad \alpha = -2\pi d \sin(\beta), \tag{13}$$

where $\vec{E}_0(\vec{r})$ is the element antenna radiation pattern, a_n, the amplitude of the n element antenna, d the separation between antennas and β the beam steering angle [16].

The beam squint observed agrees with the predicted value by theoretical calculations (1.2º at 7.5 GHz and 1.4º at 8.5 GHz) and the Sidelobe Level Ratio (SLR) is 13 dB as approximately foreseen theoretically when the antenna elements are uniformly distributed

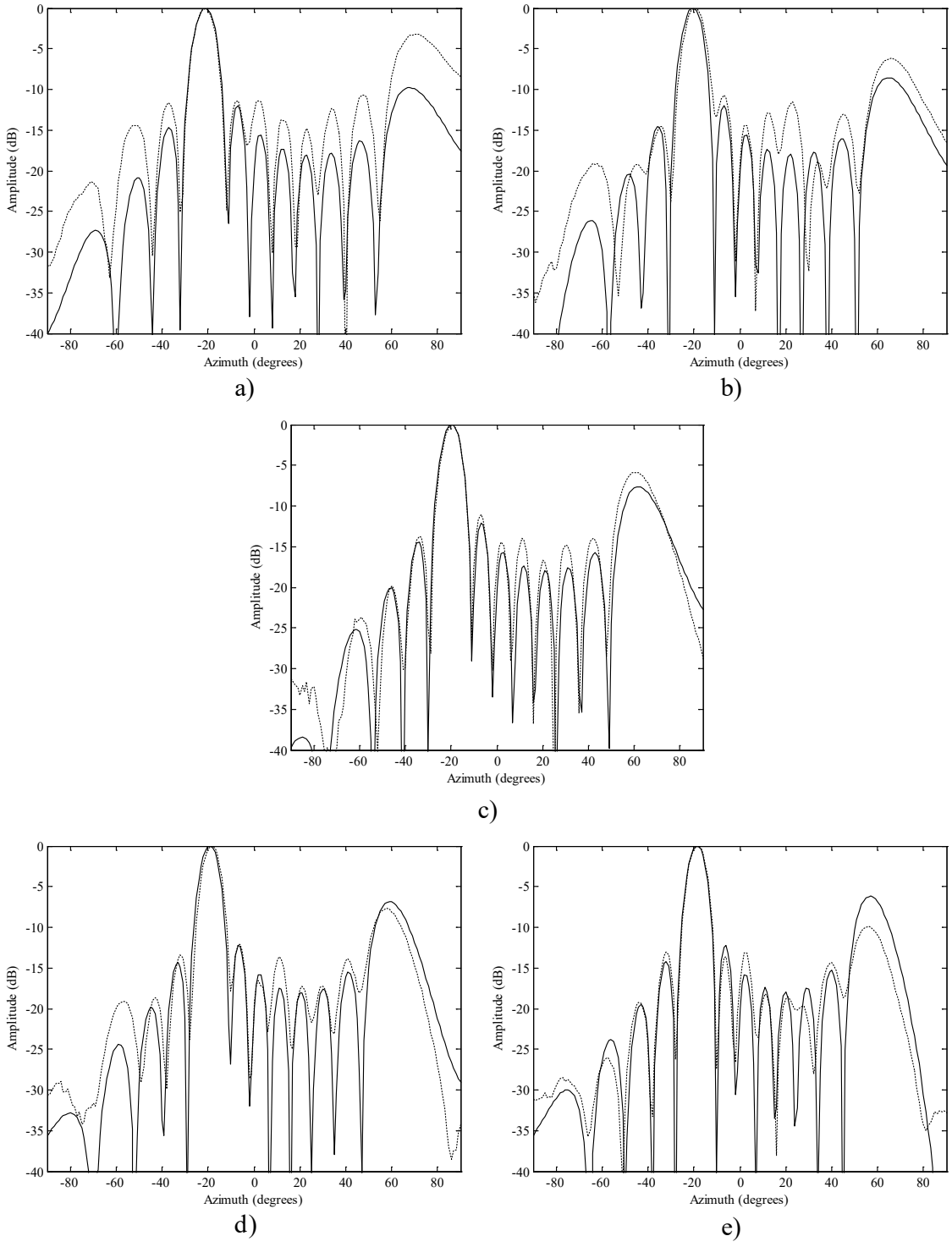

Fig. 5. Radiation pattern of the optically controlled phased array antenna steered at -20º: (solid) theory, (dotted) measured ;a) 7.5GHz, b) 7.75 GHz, c) 8GHz, d) 8.25 GHz and e) 8.50 GHz.

4.3. Multibeam capability

To show the feasibility of providing multibeam operation, the PA-NLC SLM is configured to provide two sets of phase shifts, one for antennas 1 to 4 and the other one for 5 to 8. Thus, the drive levels have been adjusted for each channel to obtain four antenna elements pointing at a fixed scan angle and the rest antenna elements pointing at a different angle at a frequency of 8 GHz. Among the different multibeam configurations, an aperture partioning to create two separate sub-apertures, i.e. two beams, has been chosen for the sake of simplicity.

The far-field patterns were measured, radiating only with a set of four elements (beam A, Fig. 6a), radiating only with the other set of four elements (beam B, Fig. 6b) and finally radiating with all the elements simultaneously (6c). In all the cases, a uniform amplitude distribution was used. The measurements were carried out at the same radiofrequency (8 GHz) although beams at different frequencies are also possible.

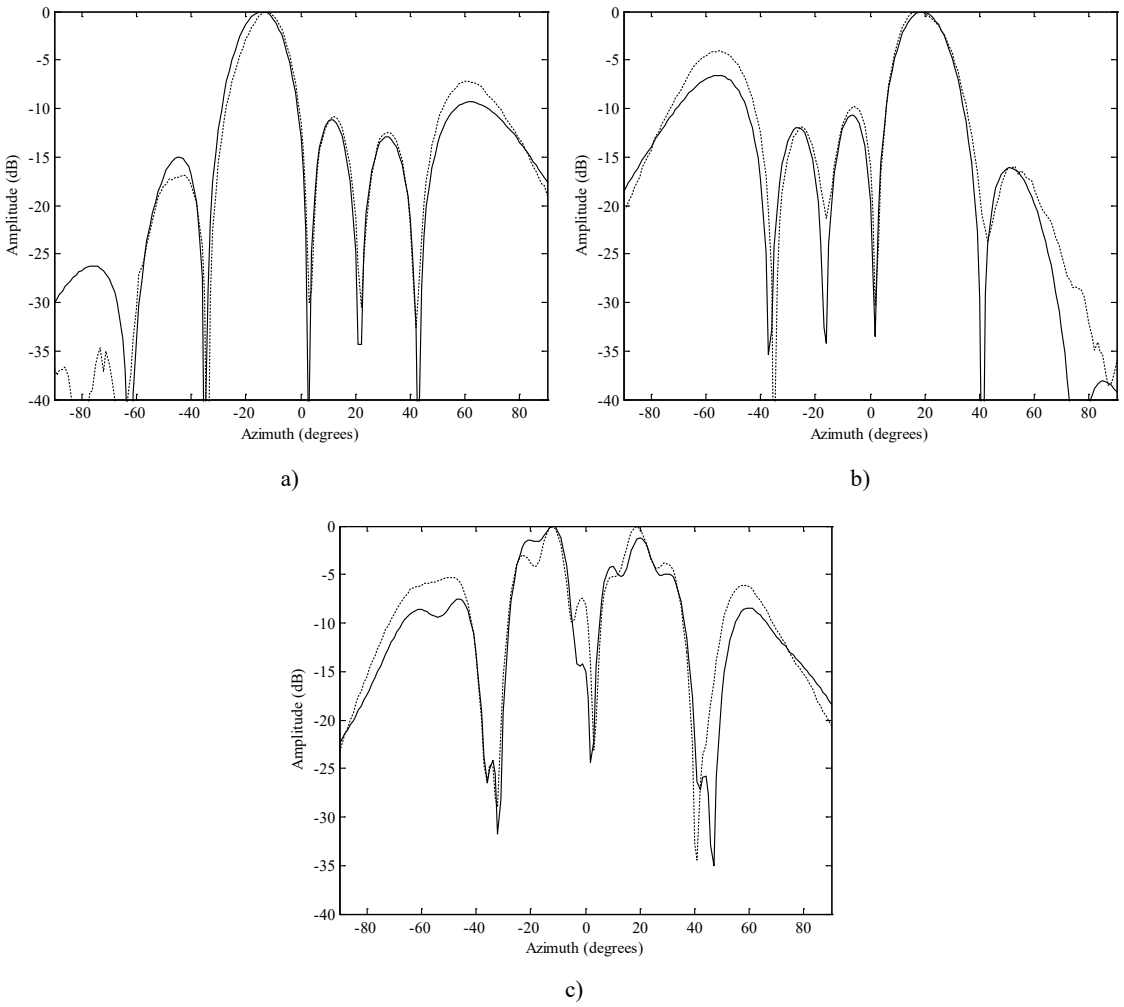

Fig. 6. Radiation pattern for the multibeam operation (-13º, 18º): (solid) theory, (dotted) measured; a) beam A, right side of array; b) beam B, left side of array c) all elements radiating simultaneously.

Beam A was adjusted to point 13º and beam B to 18º, as can be seen from Fig. 6 the radiation patterns measured agree quite well with theory. The peculiar shape of the array diagram in the case of simultaneous radiation can be attributed to the wide beamwidth of both simultaneous beams in combination with their adjacent radiation position.

4.4. Non-uniform amplitude distribution

Finally, the weighting of the antenna amplitude distribution to reduce the sidelobe level by means of the VOAs was demonstrated.

The triangular distribution of currents for an even number of elements array is defined as,

$$a_n = \begin{cases} n+1 & n < \dfrac{N}{2} \\ N-n & n \geq \dfrac{N}{2} \end{cases} \tag{14}$$

where N is the number of antennas element and n = 0,…,N-1. It has to taken into account that weights provided by (13) are not normalized [16].

Figure 7 shows the radiation pattern for a non-uniform distribution of currents on the antenna elements, in particular a triangular distribution (Table 1) in order to increase SLR. The measurement was made at 8 GHz and a 0º steering angle. As it is clearly seen, the SLR is improved up to approximately 20 dB.

	Channel 1	**Channel 2**	**Channel 3**	**Channel 4**	**Channel 5**	**Channel 6**	**Channel 7**	**Channel 8**
Relative Amplitude (dB)	-12	-6.02	-2.5	0	0	-2.5	-6.02	-12

Table 1: Weighting for Triangular distribution.

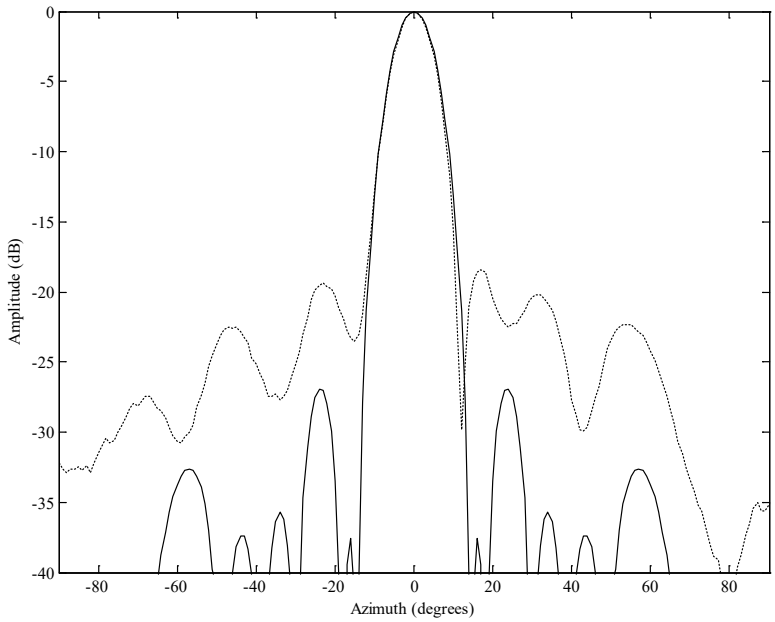

Fig. 7. Radiation pattern of the beamformer at 8 GHz when the beamsteering angle is 0º with respect to broadside and a triangular weighting is used: (solid) theory, (dotted) measured.

5. CONCLUSION

The capability of beam steering, amplitude distribution weighting and multibeam operation for tunable phase-based beamformer using MZM SSB modulation and birefringent optics has been demonstrated. Far-field radiation patterns for an eight antennas array over a frequency range of 7.5 GHz - 8.5 GHz centred at 8 GHz and for nine elevation angles within a rage of ±20º have been measured. The use of a single spatial light modulator to control many antenna elements allows the parallelization of the phase control between antenna elements with a reset speed of 70 ms. In addition, due to the availability of spatial light modulators with a large number of pixels, the architecture can be used to control several simultaneous beams as

has been demonstrated. In the case implemented, the insertion loss of the beamformer was around 12 dB.

Acknowledgements

This work has been partially funded by the European Space Agency though OBEFONE project, Generalitat Valenciana through project GV07/204 and UPV through VIDI project no.4593.

References

[1] W. Ng, A. Walston, G. Tangonan, J. Newberg, J.J. Lee and N. Bernstein, "The First Demonstration of an optically Steered Microwave Phased Array Antenna Using True-Time Delay", *Journal of Lightwave Technology*, vol. 9, pp. 1124-1131, September 1991.

[2] N. A. Riza, Editor, *SPIE Milestone Series Book* on "Photonic Control Systems for Phased Array Antennas", Vol.136, 1997.

[3] R.D. Esman, M.Y. Frankel, J.L. Dexter, L. Goldberg, M.G. Parent , "Fiber Optic Prism True Time Delay Antenna Feed", *IEEE Photonics Technology Letters*, vol. 5, no. 11, pp.1347-1349, November 1993.

[4] B. Vidal, J. L. Corral, M. A. Piqueras, J. Martí, "Optical Delay Line Based on Arrayed Waveguide Gratings' Spectral Periodicity and Dispersive Media for Antenna Beamforming Applications", *IEEE Journal of Selected Topics in Quantum Electronics*, vol. 8, no. 6, pp. 1202-1210, November/December 2002.

[5] B. Vidal, J. L. Corral, J. Martí, "Optical Delay Line Employing an Arrayed Waveguide Grating in Fold-back Configuration", *IEEE Microwave and Wireless Components Letters*, vol. 13, no. 6, pp. 238-240, July 2003.

[6] D.T.K. Tong, and M.C. Wu, "A novel multiwavelength optically controlled phased array antenna with a programmable dispersion matrix", *IEEE Photonics Technology Letters*, vol. 8, no. 6, pp. 812-814, June, 1996.

[7] M. A. Piqueras, G. Grosskopf, B. Vidal, J. Herrera, P. Sanchis, V. Polo, J. L. Corral, A. Marceaux, J. Galière, J. Lopez, A. Enard, J.L. Valard, O. Parillaud, E. Estèbe, N. Vodjdani, J. H. den Besten, F. Soares, M.K. Smit and J. Marti, "Optically Beamformed Beam-Switched Adaptive Antennas for Fixed and Mobile Broadband Wireless Access Networks", *IEEE Transactions on Microwave Theory and Techniques*, vol. 54, no. 2, pp. 887-899, February 2006.

[8] N.A. Riza, S. A. Khan, M. A. Arain, "Flexible beamforming for optically controlled phased array antenna", *Optics Communications*, 227, pp 301-310, September 2003.

[9] D. Dolfi, F. Michel-Gabriel, S. Bann, J.P. Huignard, "Two-dimensional optical architecture for time-delay beam forming in a phased-array antenna", *Optics Letters*, 16, pp 225-257, February 1991.

[10] B. Vidal, T. Mengual, C. Ibáñez-López, J. Martí, "Optical Beamforming Network based on Fiber Optical Delay Lines and Spatial Light Modulators for Large Antenna Arrays", *IEEE Photonic Technology Letters,* vol. 18, no. 24, pp. 2590-2592, December 15, 2006.

[11] P. J. Matthews, M. Y. Frankel, R. D. Esman, "A Wide-Band Fiber-Optic True-Time-Steered Array Receiver Capable of Multiple Independent Simultaneous Beams", *IEEE Photonic Technology Letters,* vol. 10, no. 5, pp. 722-724, May, 1998.

[12] N.A. Riza, "an Acoustoptic-Phased-Array Antenna Beamformer for Multiple Simultaneous Beam Generation", *IEEE Photonics Technology Letters*, vol. 4, no. 7, pp. 807-809, July 1992.

[13] U. Efron, "Spatial Light Modulator Technology", *Ed. Marcel Dekker*, 1995.

[14] O. Kobayashi, H. Ogawa , "A Liquid-Crystal Control, Coherent Type Optoelectronic Phased Array Antenna Beam Forming Network Using Polarization Multiplex Optical Heterodyning", *IEICE Trans Electron*, vol. E79-C, no. 1, pp. 80-86, Jan 1996.

[15] G. H. Smith, D. Novak and Z. Ahmed, "Technique for optical SSB generation to overcome dispersion penalties in fibre-radio systems", *Electronics Letters*, vol. 33, no. 1, pp. 74-75, 2nd January 1997.

[16] C. A. Balanis, "Antenna Theory". *John Wiley* 2005.